Comparison of Cornea Deformation Under Physiological Inflation Conditions

T. D. Nguyen, [a] R. E. Jones, [c,*] B. L. Boyce [b]

[a] *Department of Mechanical Engineering, Johns Hopkins University, 125 Latrobe Hall, Baltimore, MD 21218, USA*

[b] *Mechanics of Materials Department, Sandia National Laboratories, P.O. Box 0969, Livermore, CA 94551, USA*

[c] *Microsystems Materials Department, Sandia National Laboratories, P.O. Box 5800, Albuquerque, NM 87123*

Abstract

Key words: cornea, viscoelasticity, creep, mechanical behavior, tissue mechanics
PACS:

1 Introduction

talking points:

(1) sources of discrepancy between tension and bulge, e.g. matrix properties (shear), recruited fibril density, thickness. Compare experiments with tension parameter predictions and bulge fitted parameters. Note evolution during preconditioning is roughly 30% versus 100% for tension.

Simulations: compare apex displacement for cycle C for 3.6-8 kPa or 0-8 kPa or 0-32 kPa

(2) viscous effects : can they be predicted using refitted elastic parameters and tension-derived viscous parameters?

(3) weak periphery-strong center theory of cornea deformation. Does the holder obscure the validity of this observation with respect to *in vivo*?

* Corresponding author.
Email address: rjones@sandia.gov (R. E. Jones,).

Simulations: show the effects of changing the assumed fibril distribution, e.g. add more fibrils to the center

Observations: with an in-plane isotropic distribution the displacements I get still seem to be larger at the edge and flatter in the center. I think this is largely controlled by the matrix shear modulus i.e. the lamellae are being sheared at the fixture and the distribution doesn't matter as much in out-of-plane shear.

(4) anisotropy effects: due to symmetry of distribution, geometry, loading, boundary conditions/fixture.

Simulations: use a "human"/circular cornea and compare : iso distribution with same fibril density, assumed distribution with fixed edges, assumed distribution with free radial expansion

Observations: (a) with a free edge and without the sclera the limbus tends to contract radially with applied pressure i.e. it is put into compression. (b) with an attached (pseudo)sclera/globe the limbus tends to expand radially with applied pressure i.e. the reinforcing circumferential fibrils are loaded (in tension). (c) in both cases, and probably in general, the first principle stress (radial?) is approximately uniform across the cornea, the second has a gradient through the thickness and the third a gradient radially. ergo it seems like we cannot simultaneously isolate the cornea and load it physiologically without mimicking the expansion of the globe under pressure.

(5) clinical relevance/application : e.g. applanation in tonometry, relaxation during keratotomy surgery. Also, look at change in focal length and refractive power with excursions from IOP. (Talk to S. McLeod.)

to do:

- agree on one bovine and one human mesh (and check into repository)
- agree on a fibril distribution

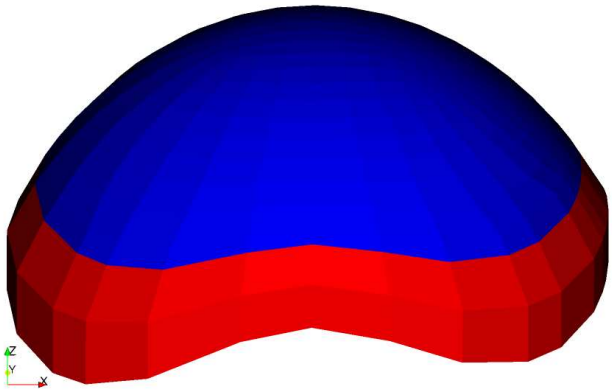

Fig. 1. Finite element mesh of the cornea, the red regions are held fixed, to approximate the permeation of the glue into the stiffer schleral tissue, and the inner surface is pressurized

2 Results

The Pressure-Dependent Vertical Displacement Field. The present section describes features found at maximum pressure when the total displacements are at or near their maximum. More detail can be found regarding the pressure-dependent evolution of the displacement field as shown in Figure **??**. At the minimum reference pressure of 0.1 kPa, the cornea is in its reference configuration and there is no U,V or W displacement. At a pressure of 0.7 kPa, which is <10% of the maximum pressure and <30% of typical bovine IOP, the cornea appears to have a smoothly-graded nearly symmetric displacement field. At this sub-IOP pressure, the cornea has already deformed quite substantially: the maximum W-displacement in the central cornea of $\approx 0.55mm$ is more than half of the final deformation that will be achieved at a maximum pressure of 8 kPa. By a pressure of 2.4 kPa, nearing typical bovine IOP, the shape of the deformation contours has transformed significantly with the deformation contours now more rectangular and stretched along the inferior-superior axis rather than the nasal-temporal axis found at 0.7 kPa. The characteristic contour shapes that emerge at pressures near IOP persist to higher pressures and are still evident at 7.4 kPa. At the pressure of 2.4 kPa, the cornea has already experienced >80% of its total W-displacement. The displacement profile at a pressure of 6.1 kPa is nearly identical to that at 7.4 kPa. These observations highlight the well-known nonlinear elastic response of the cornea: it is much stiffer at pressures near IOP and above than it is in the fully relaxed state.

Statistically Averaged Displacement Response. The displacement fields for individual cornea samples do not exhibit regular, symmetric contours indicative of a possible lack of isotropy and/or property homogeneity. Since there was some variability from sample-to-sample, a composite average displacement field for all 9 tests under nominally identical conditions was constructed. [REJ: DESCRIBE LAGRANGE TO EULER MAP USED IN THE AVERAGING.] The resulting initial configuration and displacement field is shown in Figure 2 and Figure 3, respectively.

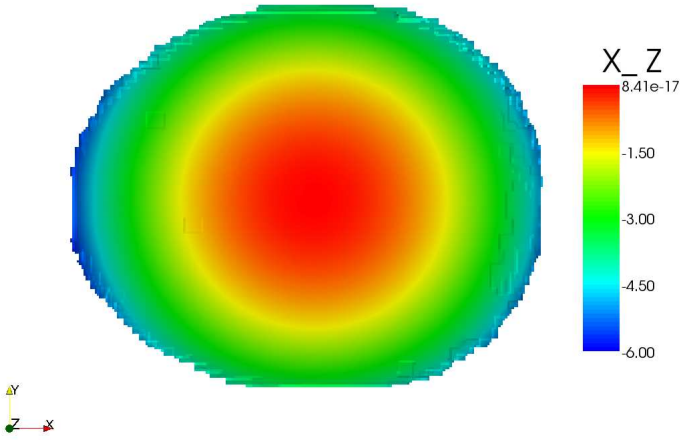

Fig. 2. Averaged configuration at 3.6 kPa and after preconditioning

As another way to condense the rich dataset, a scalar W-displacement value was extracted at each timestep of the 9 identical tests. The W-displacement values were taken from the central cornea at the highest point of the original reference configuration. This provides an apex displacement value that can be readily examined as a function of time or pressure. The averaged apex displacement for the 9 identical tests is shown in Figure 4. In this figure the three different pressurization rates, i.e. cycles A, B, and C, are compared directly corresponding to pressurization rates of 0.036, 0.0045, and 0.29 kPa/s, respectively. It is interesting to note that there is significantly less sample-to-sample scatter in this inflation data than in preceding tensile experiments **?**. At all pressure-rates the cornea displays viscoelastic hysteresis, but only a small degree of non-linearity compared to the tensile results. This important feature will be analyzed in more detail in the Discussion section.

Since cycles A and D are nominally identical, both at a ramp rate of 0.036 kPa/s, one can assess the repeatability of the tests. Average apex displacement is plotted as a function of pressure for both of these cycles in Figure 5. As intended, the two cycles result in nearly identical behavior, well beyond statistical distinguishability. [REJ: ADD ERROR BARS?] This suggests that the cornea loading condition returns to a well-defined reference state for each of the cycles, and that any possible time-dependent or cycle-dependent evolution of the material does not affect the resulting mechanical response.

Apex displacement can also be examined as a function of time. This is especially interesting for the constant-pressure creep and constant-volume relaxation cycles, E and F. The average response for these two loading cycles are shown in Figure 6. The creep behavior at a constant pressure of 8 kPa quickly reaches a steady-state creep rate on the linear timescale. The creep-rate does not diminish with increasing time. [REJ: DO WE SHOW THIS?] On a logarithmic timescale, the cornea creep rate is growing exponentially, similar to the tensile

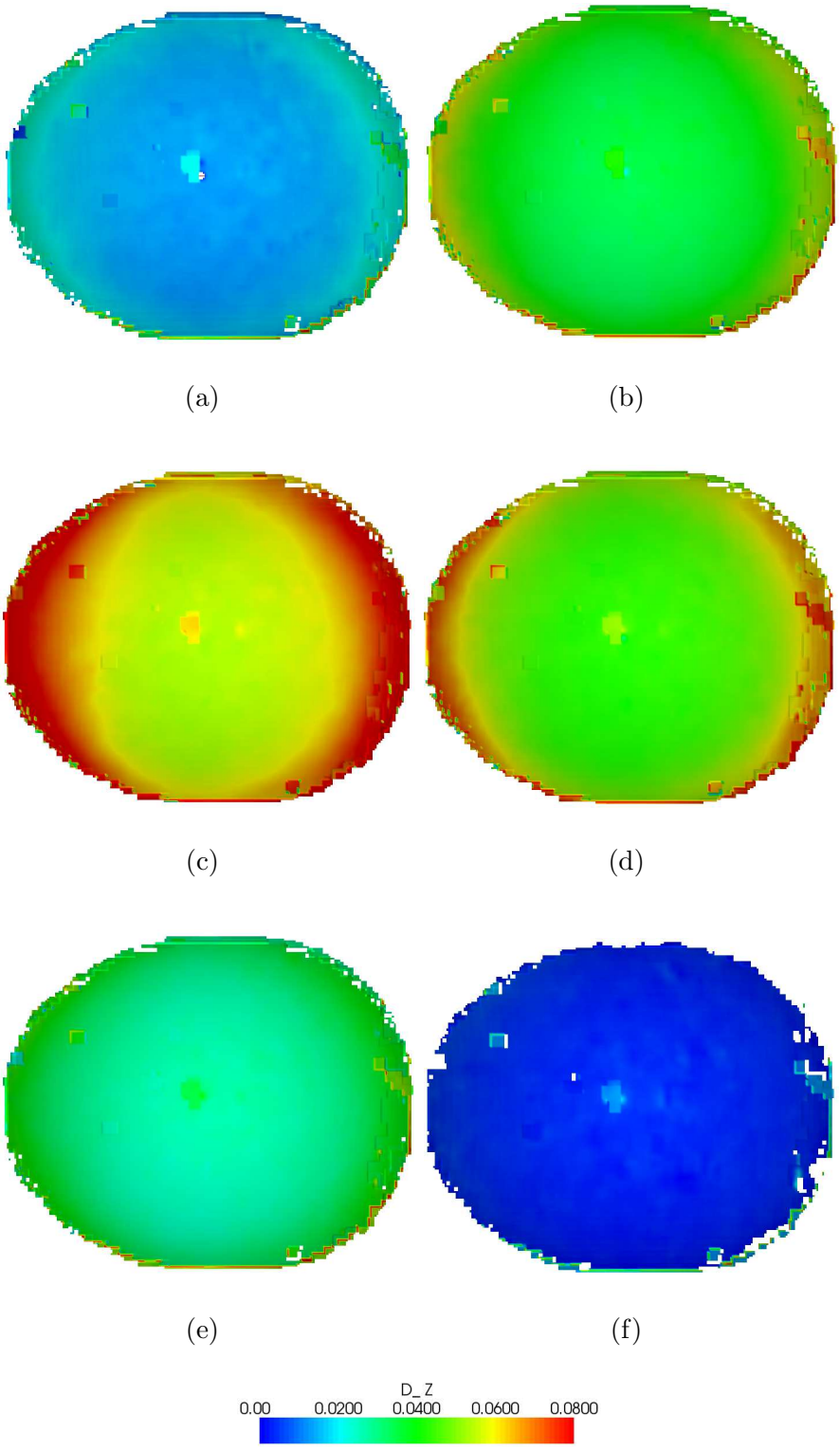

Fig. 3. Cycle A : averaged displacements at t= (a) $11s$, $5.07\,kPa$; (b) $22s$, $6.53\,kPa$; (c) $33s$, $8.00\,kPa$; (d) $44s$, $6.53\,kPa$; (e) $55s$, $5.07\,kPa$; (f) $66s$, $3.60\,kPa$;

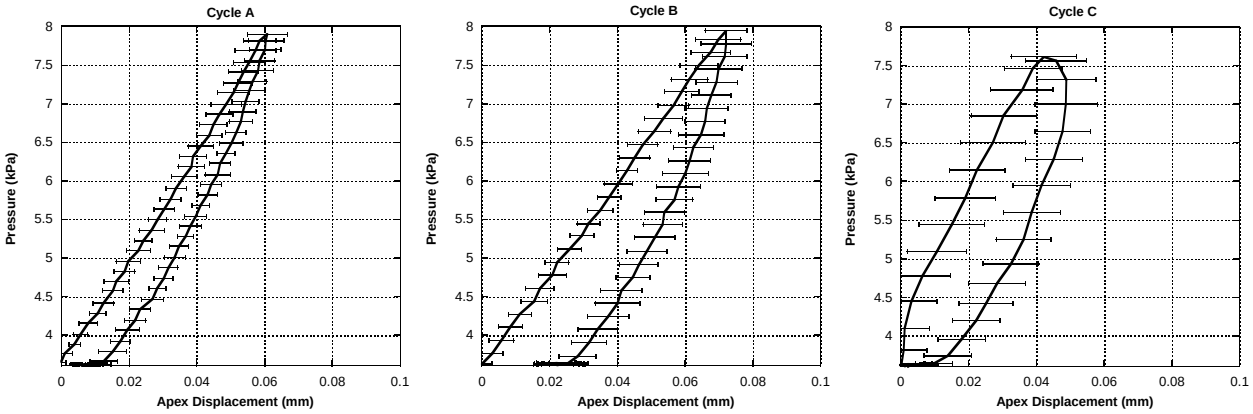

Fig. 4. The average apex displacement at a function of applied pressure during triangular loading cycles A, B, and C, corresponding to pressurization rates of 0.036, 0.0045, and 0.29 kPa/s, respectively. Error bars indicate 1 standard deviation.

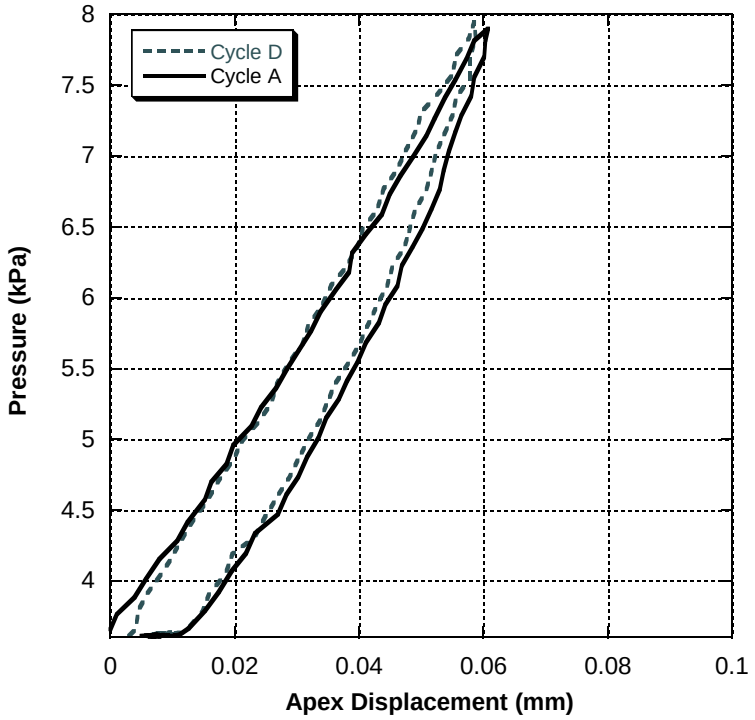

Fig. 5. A comparison of average apex displacement for two nominally identical cycles in the loading regimen.

creep curves for the higher tensile stresses of 350 and 500 kPa shown in Figure **??**, which suggests activation of multiple creep elements at different timescales **?**. The pressure and apex displacement evolution at constant volume shows expected relaxation of the pressure. Also, as expected, the apex displacement continues to creep since the pressure continues to be well above the rest-state, i.e. 3.6 kPa.

Local Deformation: Central Cornea and Limbus. The ability to extract local displacement vectors allows the evaluation of spatially disparate response. To compare the deformation

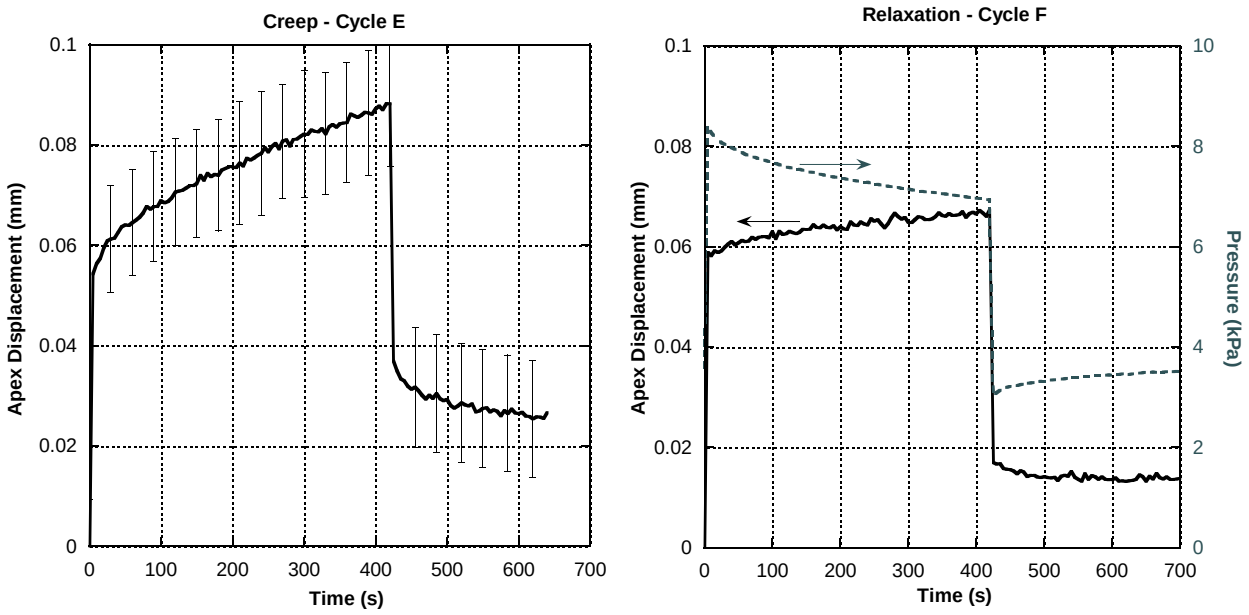

Fig. 6. Creep and relaxation during cycles E and F, respectively.

of the central cornea to deformation around the limbal periphery, displacement values were extracted from positions midway between the corneo-scleral junction and the apex of the cornea, along each of the four directions: nasal, temporal, inferior, and superior. These mid-peripheral displacements were compared directly to the apex displacement for one specific loading cycle in Figure 7. While the pressure-displacement profile for a single specimen is not as smooth as the averaged response, nevertheless a specific trend is obvious: The displacement values at the mid-periphery points account for $\approx 90\%$ of the displacement that occurs at the apex. In other words, the central cornea largely retains its shape during deformation. As a corollary, the pressure-driven deformation is largely accommodated in the limbus of the cornea. [REJ: WE SHOULD COLLECT ALL RESULTS FOR THIS CONCLUSION HERE.]

The Response of the Cornea over a Wider Pressure Range. While the preceeding results correspond to pressures in the range of 3.6-8 kPa, i.e. within the range of physiologically plausible pressures experienced by the bovine species, inflation experiments were also performed over a much wider pressure range from 0.7-32 kPa. From these results, a few key cycles were plotted in Figure 8. Cycles A and B exhibit a dramatically nonlinear or J-shaped pressure-displacement response. It is interesting to note that the knee in the response is located in the vicinity of $\approx 2kPa$, at the onset of typical intraocular pressures. Also note, that this wide-range data supports the notion that the material response is approximately linear over the smaller physiologic range of 3.6-8 kPa, as was observed in the previously described experiments. While this wider range is outside the realm of physiologically relevant pressures, it provides a connection to commonly observed J-shaped stress-strain curves found in the literature. The creep response at a constant pressure of 32 kPa showed a constant creep rate on a linear timescale, similar to that observed at a creep pressure of 8 kPa, here again suggesting the activation of multiple creep mechanisms and different timescales.

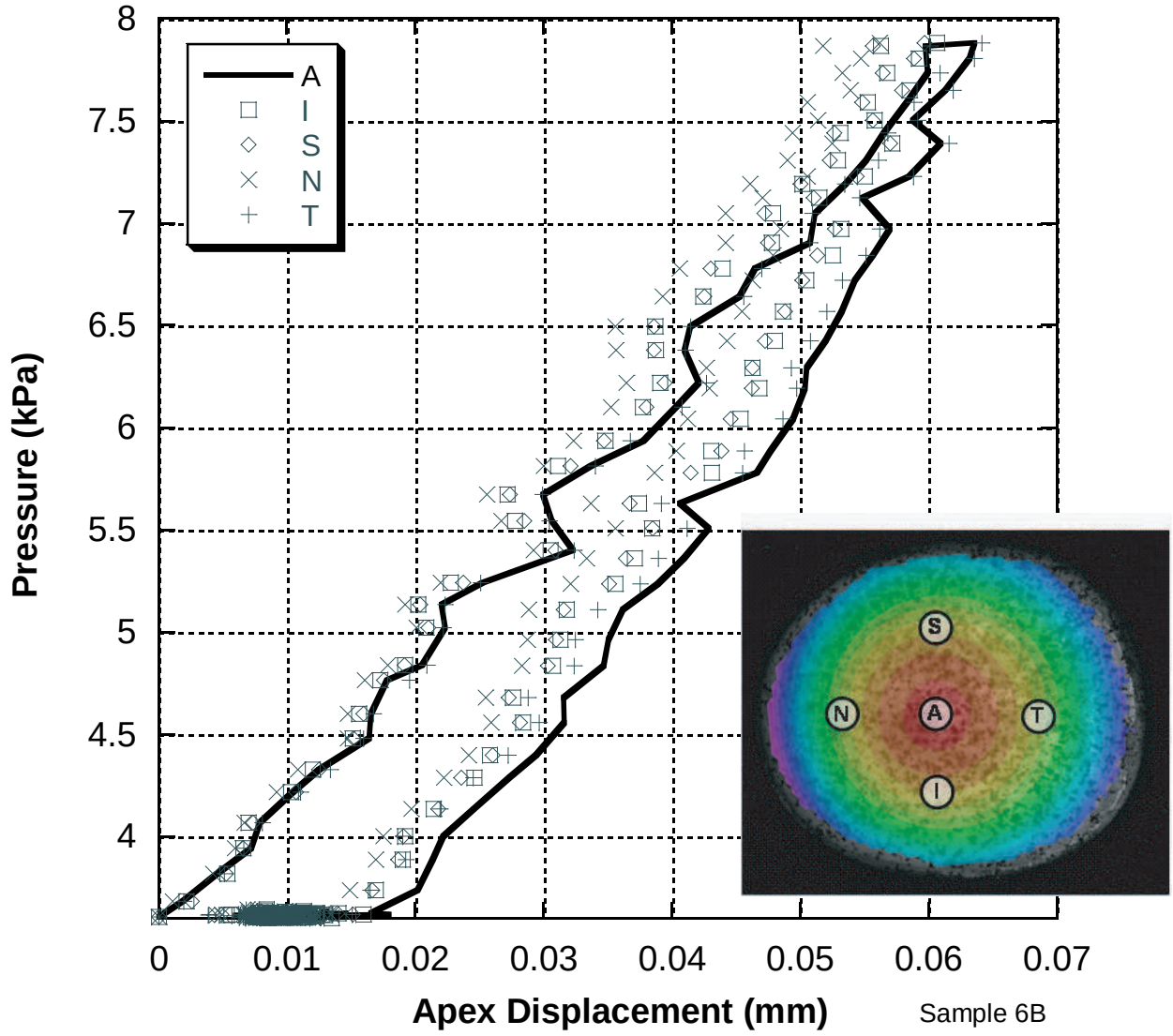

Fig. 7. Local mid-periphery displacement values compared to the apex displacement.

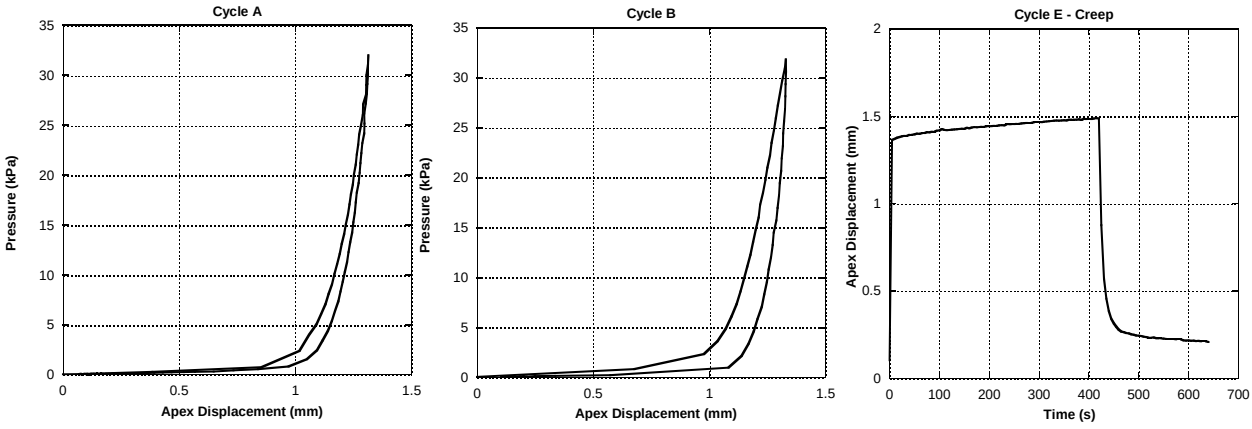

Fig. 8. Response to pressures $0 - 32\,kPa$.

3 Discussion

Predictability of Inflation Experiments. Using the finite element mesh constructed from DIC data and the constitutive model described in **?**, the response of the cornea to the programmed pressure excursions was simulated. Figure 9 shows how the response of the cornea changes with increasing pressure. Specifically, it clearly demonstrates large deformation and subsequent rapid change in stiffness as the collagen fibrils go from slack to taut. It is also important to note that the higher stress behavior is similar, i.e. after the weak low stress response is removed, in all three types of tests. [REJ: SHOW THIS MORE CONCLUSIVELY] Since the model described in **?** was conditioned on tensile data starting from the perceived knee in the response, the parameters obtained from the tension fits should correlated well with the data in the 3.6-8.0 kPa regimen. However, referring to Figure 10, it is clear that the apex displacement is overpredicted by roughly a factor of 6. There are a number of plausible sources for this error, including: (a) the matrix bulk and shear moduli assumed in the tension work are not representative of the cornea (and the inflation response is relatively more sensitive to these parameters than the tension fit). (b) the intact fibril density was underestimated in the tension experiments due to loading only the unsevered fibrils, (c) the thickness of the cornea was underestimated by the direct measurements, [REJ : INCLUDE A TABLE OF THICKNESS MEASUREMENTS?] which would effectively be an underestimation of both the matrix and fibril response. Sensitivity studies show that the inflation response is much more sensitive to the matrix parameters than the tension response. However, the sensitivity to the fibril response in inflation is much greater than the matrix response at the fitted values, as expected. Figure 10 shows the response of the same model but fortified with 4x the density of fibrils. The response is quite comparable to the data, but it is hard to attribute all of the error to this cause since it implies loading only 1/4 of the fibrils in the tension experiment. [REJ: THIS IS CONFOUNDED BY THE FACT THAT IS HARD TO COMPARE PRECISELY THE SLACK/NO-SLACK POINTS IN THE TENSION VERSUS BULGE EXPERIMENTS.]

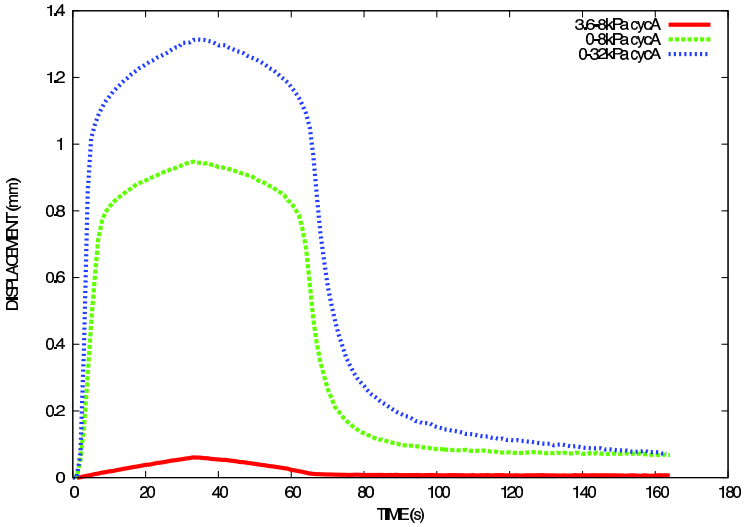

Fig. 9. Comparison of the apex displacement for the three regimens.

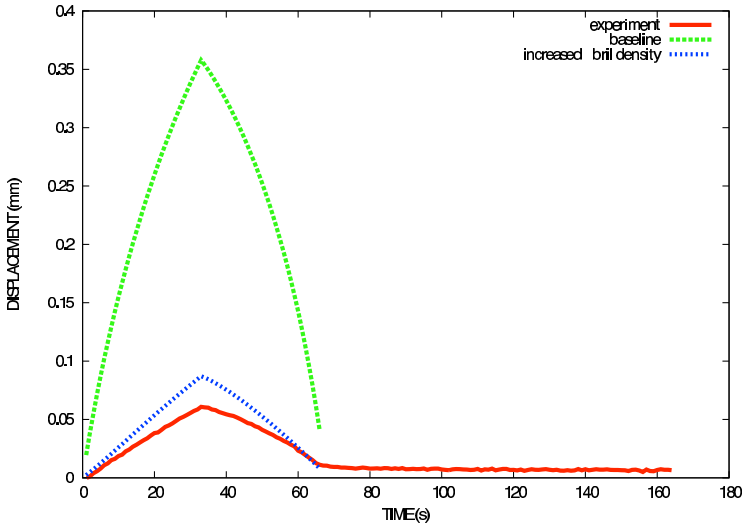

Fig. 10. Comparison of the experimental apex displacement to the nominal model and one with increased fibril density.

The full field DIC displacement data also provided a means of comparing the effects of fibril density on deformation. Figure 11 shows the assumed fibril density across the cornea, and is adapted from the work **?** on human corneas

$$\begin{aligned}\phi(r,\theta) = d_{\text{central}} R(r, R_{\text{NT-IS}}, R_{\text{periphery}})(\cos^8\theta + \sin^8\theta + 0.451) \\ + d_{\text{periphery}} R(-r, R_{\text{limbus}}, R_{\text{periphery}})(\sin^8\theta + 0.720)\end{aligned} \tag{1}$$

where (r,θ) are polar coordinates in the NT-IS plane, d_{central}, d_{central} are densities in the central cornea and periphery, and $R(x, x_1, x_2)$ is ramp function that is zero for $x < x_1$, one for $x > x_2$ and linear in between. It is clear from Figure 12 that the high density of fibrils in the center cornea provides the stiffness necessary to maintain its shape, while the largest deformations occur at the periphery, much like in Figure 3c. However, there is no apparent effects of the anisotropy in fibril density in the central cornea, where most fibrils run in the NT and IS directions. An explanation of this observation is predicated on the fact that the cornea under inflation is nominally in an equibiaxial mode of deformation and, at least at small stretches, the corresponding tangent modulus of the fibril component of the model

$$\mathbb{C} \;\approx\; \frac{1}{2\pi}\int_{-\pi}^{\pi} \frac{\partial^2 w_{fibril}}{\partial(\lambda_{\mathbf{M}}^2)^2}\bigg|_{\lambda=1} \mathbf{M}\otimes\mathbf{M}\,\phi\,d\theta \tag{2}$$

is approximately isotropic in plane since the fibril stiffness $\frac{\partial^2 w_{fibril}}{\partial(\lambda_{\mathbf{M}}^2)^2}$ is independent of θ in the reference configuration. [REJ : NEED MORE BACKGROUND HERE.] Figure 13 illustrates this point for the deformation of the central cornea only. The deviations from isotropy are on the order of 1/100th the mean displacements.

Application of the Model to Applanation of Cornea during Tonometry. As an application of the geometric and constitutive model to a problem of clinical relevance, a simulation of glaucoma screening via tonometry was constructed. In this common diagnostic test, a flat punch makes contact with the anterior surface of the cornea measuring the internal pressure

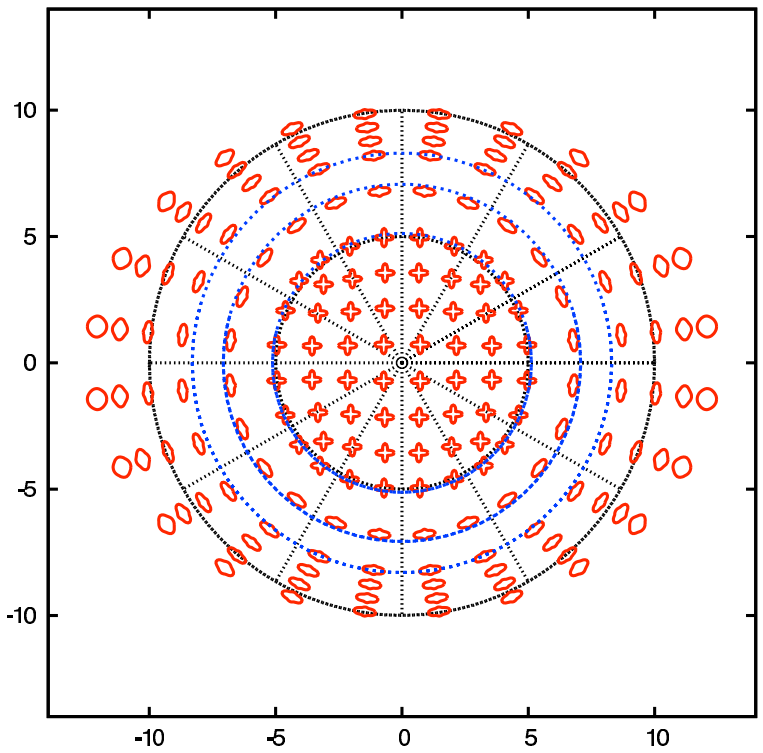

Fig. 11. Fibril density at selected points across the cornea

of the eye indirectly through the cornea. Given the apparent viscous effects that are intrinsic to the cornea, not to mention those associated with other tissues of the globe and the aqueous humor, the conjecture was that the rate of loading would affect the reaction force measured by the instrument. Although the full globe is not modelled nor are the fluid effects, they are mimicked in part in the simulation by a constant volume constraint under the cornea. A cylindrical flat-ended punch was made to approach the cornea at two different loading rates : $1.0\,mm/s$ and $10.0\,mm/s$. A typical displacement of anterior surface is shown in Figure 14 and Figure 15 shows that the reaction force after $10s$ is different by $< 2\%$. This finding gives confidence to the accuracy of this common test.

4 Summary and Conclusions

The present study employed a newly developed cornea inflation and deformation mapping scheme to examine the viscoelastic deformation of the cornea under conditions that closely match *in vivo* conditions. This physiologically-inspired study revealed aspects of cornea deformation that can not be readily gleaned from most *ex situ* experiments. It is clear from these experiments that the structure of the cornea is tailored to operate under positive pressures in the realm of intraocular pressures. At pressures lower than the typical intraocular range, the response of the cornea is much less stiff, almost certainly due to slack collagen fibrils which are perhaps readily buckled in the relatively weak matrix. Another important observation from this study is that the central cornea deforms very little over a physiologic

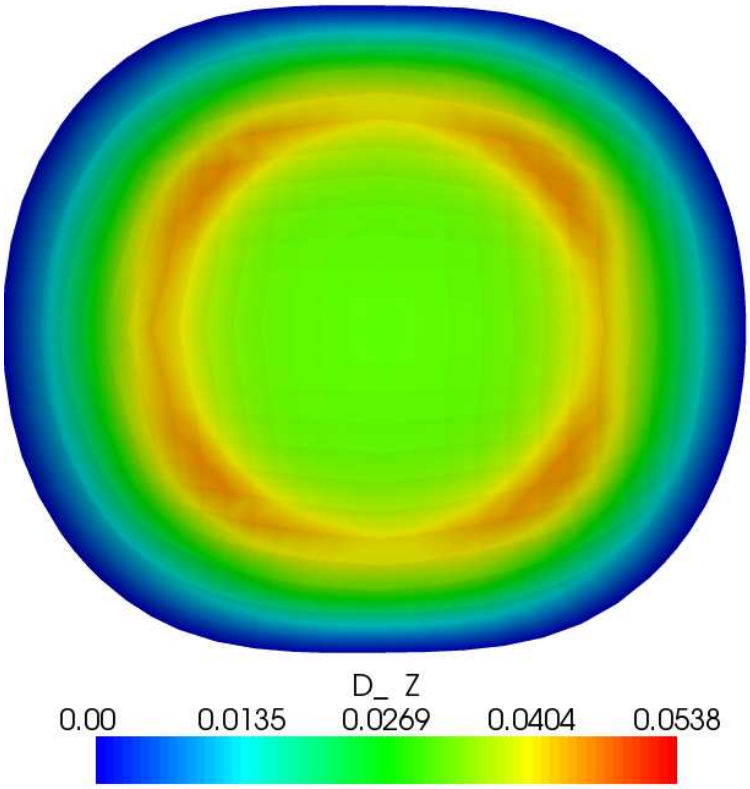

Fig. 12. Simulated vertical displacements showing strong center cornea and relatively weak periphery

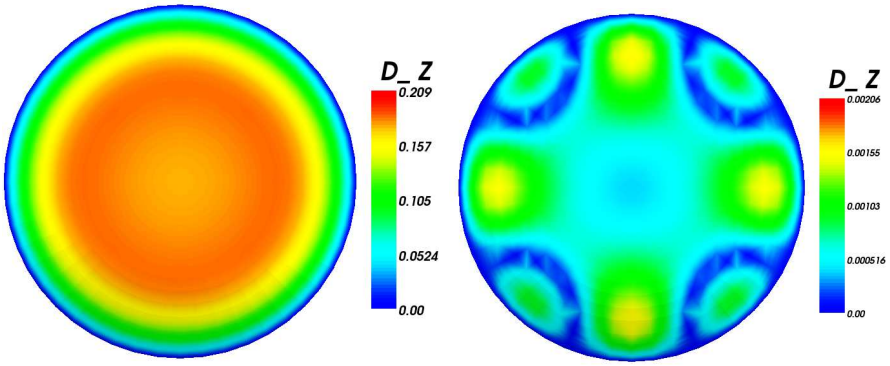

(a) (b)

Fig. 13. Displacements of the central region only: (a) total displacements for a primarily NT-IS oriented fibril density, and (b) the deviations of this deformation map with an isotropic (in-plane) arrangement of fibrils

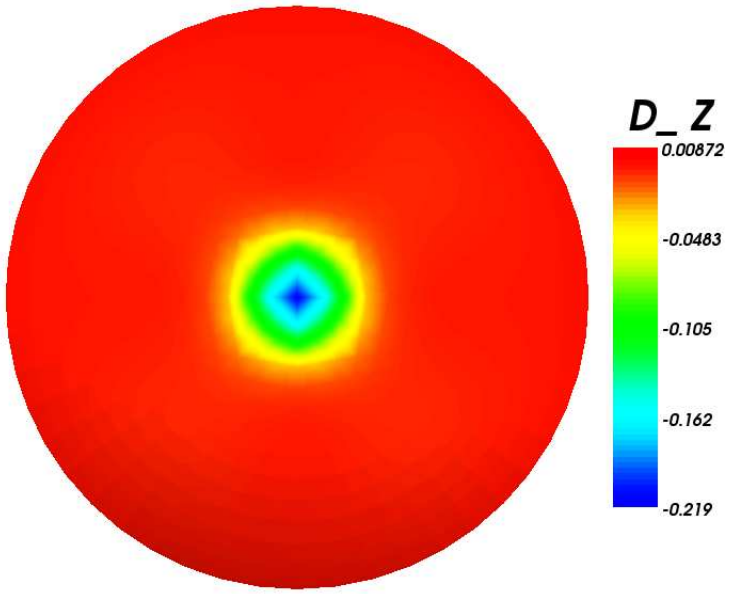

Fig. 14. Applanation of a human cornea

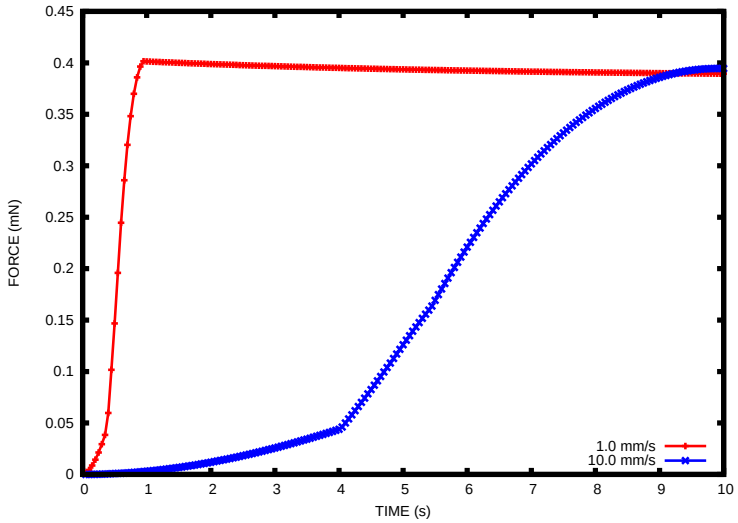

Fig. 15. Applanation reaction force due to loading at $1.0\,mm/s$ and $10.0\,mm/s$.

pressure range. This feature is attributed to the circumferential alignment of limbal fibrils which are more compliant along the radial axis than the radially-aligned central cornea fibrils. The result of this radially stiff central cornea is that the central cornea retains its shape and optical power during pressure excursions. Another finding of clinical importance is the cornea's response, over the physiological pressure range and the timescales considered, may be reasonably approximately as linear and relatively free of hysteresis. While an original emphasis of this program was to examine the non-linear viscoelastic response of the cornea, which had been largely ignored in the literature, the inflation results suggest that linearity is a reasonable first-order approximation *under physiologic conditions*. In addition, the under physiologic conditions, the cornea appears to have multiple creep modes active, a phenomenon that was only evident in tensile results at high mean stress or long timescales.

While the present study has emphasized physiologic conditions, the timescale of these experiments was necessarily short, less than 1 hour. The extrapolation of these results to longer term events such as glaucoma and other disease processes is questionable. However, the findings of this work have significant relevance to shorter timescale processes such as corrective surgery and screening tests. Future work to examine longer term physiologically-relevant mechanical evolution in cornea properties will almost certainly require *in vivo* experiments, such as by tonometry.

Acknowledgments

This work was funded by the Laboratory Directed Research and Development program at Sandia National Laboratories and its support is gratefully acknowledged. Sandia is a multiprogram laboratory operated by Sandia Corporation, a Lockheed Martin Company, for the United States Department of Energy under contract DE-ACO4-94AL85000.